



Joint Waveform and Beamforming Designs for RIS-ISAC Systems

Rang Liu

March 13, 2024

Rang Liu

Center for Pervasive Communications and Computing

University of California, Irvine, CA 92697, USA

E-mail: rangli2@uci.edu

Website: <https://rangliu0706.github.io/>



Education:

Ph.D. Dalian University of Technology, Dalian, China 2018 - 2023

B.S. Dalian University of Technology, Dalian, China 2014 - 2018

Research:

Integrated sensing and communications (ISAC)

Reconfigurable intelligent surfaces (RIS)

Symbol-level precoding

Physical layer security

CONTENT

- 1 Introduction of RIS-ISAC**
- 2 General System Model**
- 3 Joint Designs for RIS-ISAC**
- 4 Conclusions and Future Directions**

01

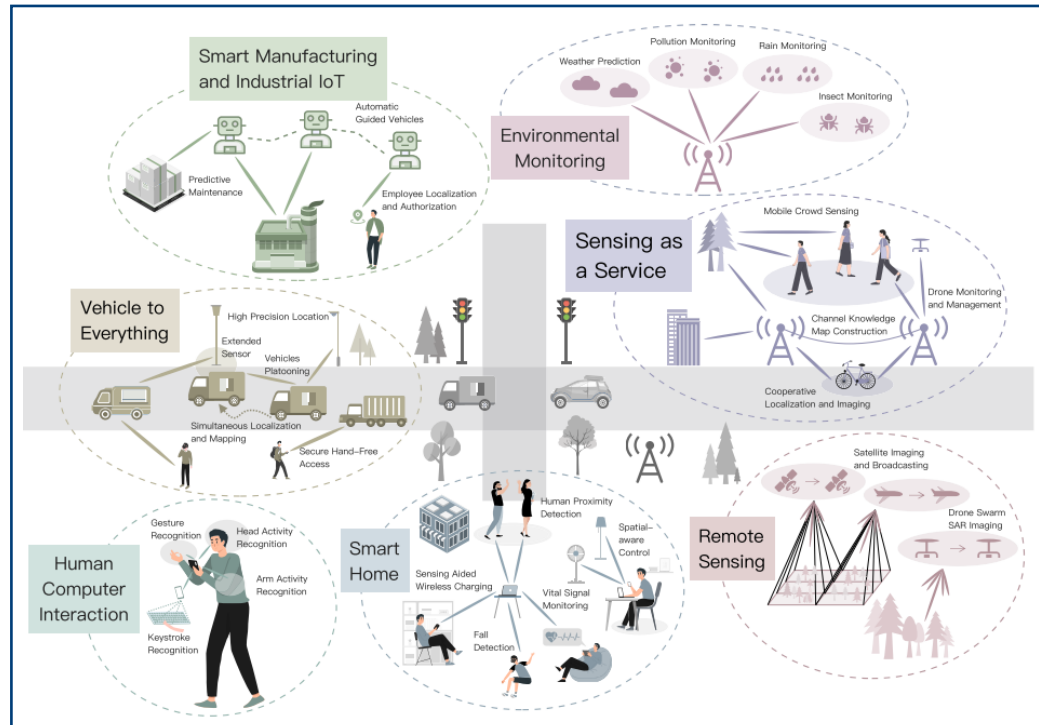
PART ONE



Introduction of RIS-ISAC



Integrated Sensing and Communications (ISAC)



- Spectrum sharing
- Colocated hardware
- Unified waveform
- Joint signal processing
- High efficiencies
- Performance trade-off

Fig. 1. ISAC technology for future wireless networks [1].

High-quality ubiquitous communications and high-accuracy sensing!

[1] F. Liu, et al., "Integrated sensing and communications: Toward dual-functional wireless networks for 6G and beyond," *IEEE J. Sel. Areas Commun.*, vol. 40, no. 6, pp. 1728-1767, Jun. 2022.

Reconfigurable Intelligent Surfaces (RIS)

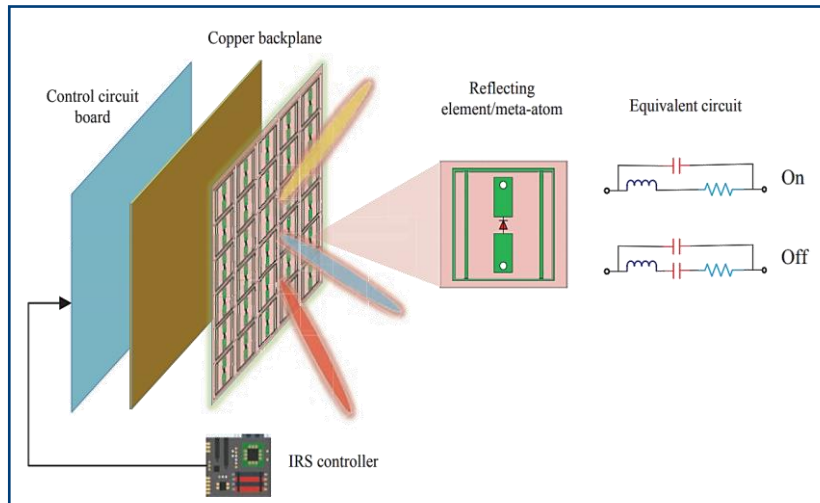


Fig. 2. Architecture of RIS [2].

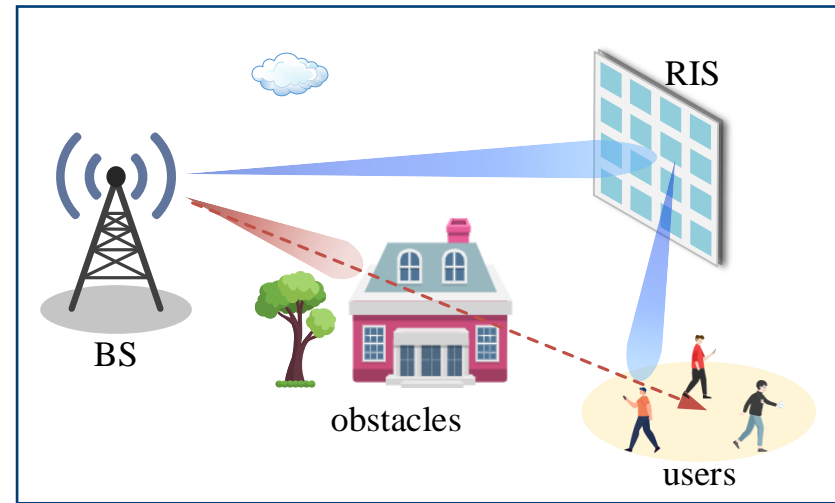


Fig. 3. A RIS-aided communication system.

- Passive reflection elements
- Adjusting the parameters of EM waves

- Cost-effective and hardware-efficient
- Reshaping radio environment

Low-cost, wide-coverage, and high-quality wireless networks!

[2] Q. Wu and R. Zhang, "Towards smart and reconfigurable environment: Intelligent reflecting surface aided wireless network," *IEEE Commun. Mag.*, vol. 58, no. 1, pp. 106-112, Jan. 2020.

Background of RIS-ISAC

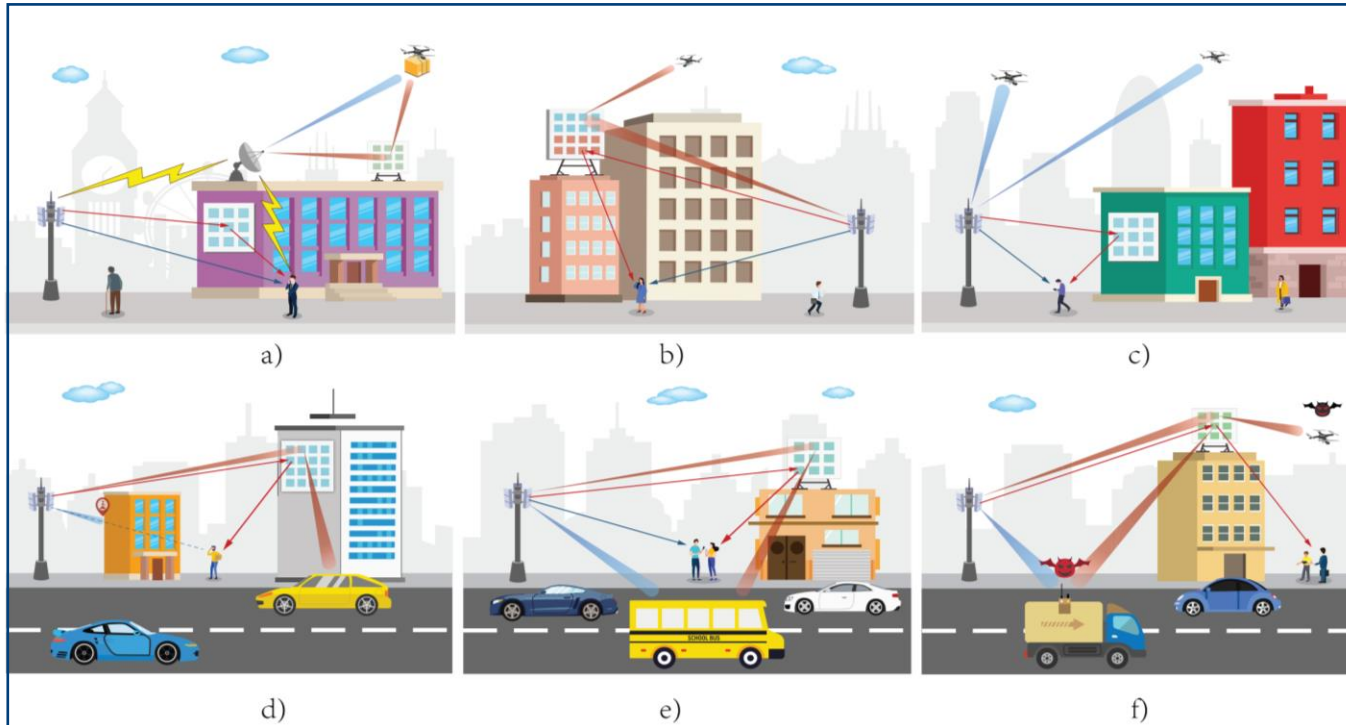
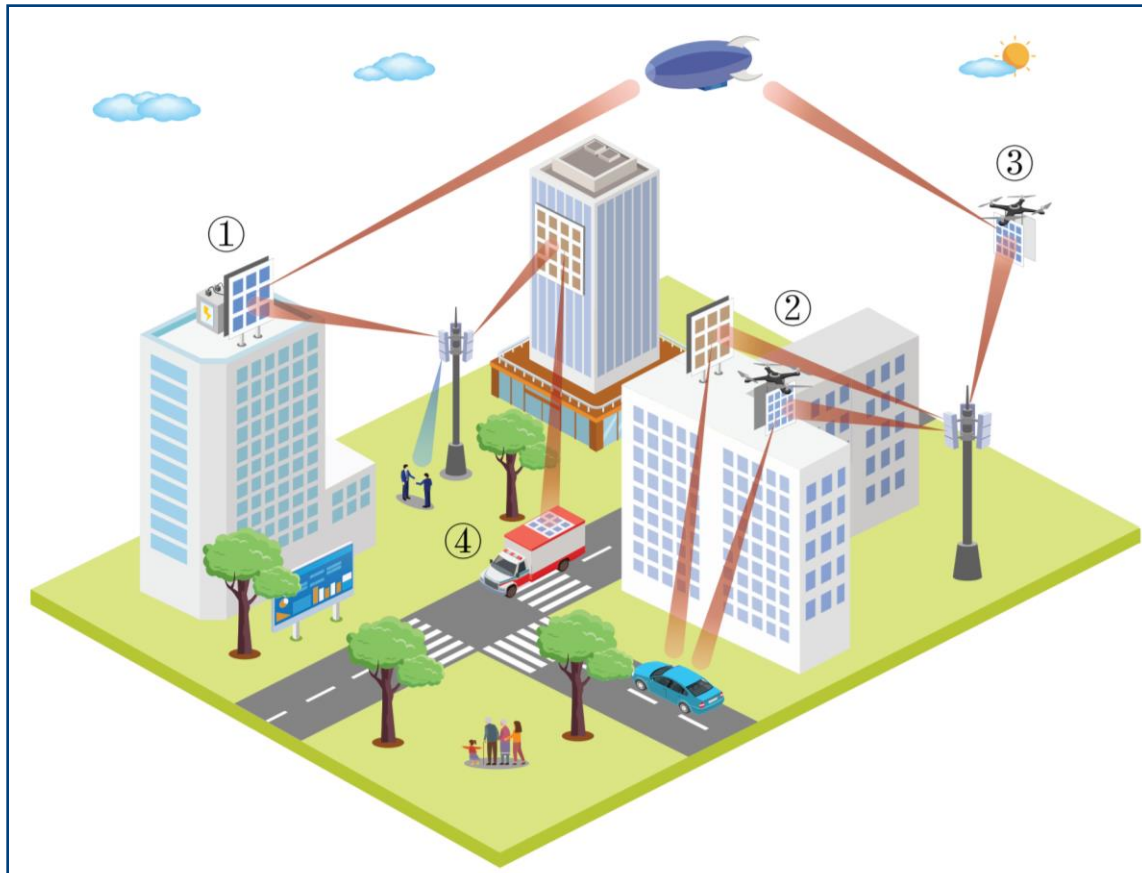


Fig. 4. Typical applications of RIS in ISAC systems [3].

Virtual LoS link
New dimension

- [3] Rang Liu, M. Li, H. Luo, Q. Liu, and A. L. Swindlehurst, "Integrated sensing and communication with reconfigurable intelligent surfaces: Opportunities, applications, and future directions," *IEEE Wireless Commun.*, vol. 30, no. 1, pp. 50-57, Feb. 2023.

Background of RIS-ISAC



- active RIS
- multiple RISs
- UAV-mounted RIS
- target-mounted RIS

Fig. 5. Various RIS deployments in ISAC systems [3].

Background of RIS-ISAC

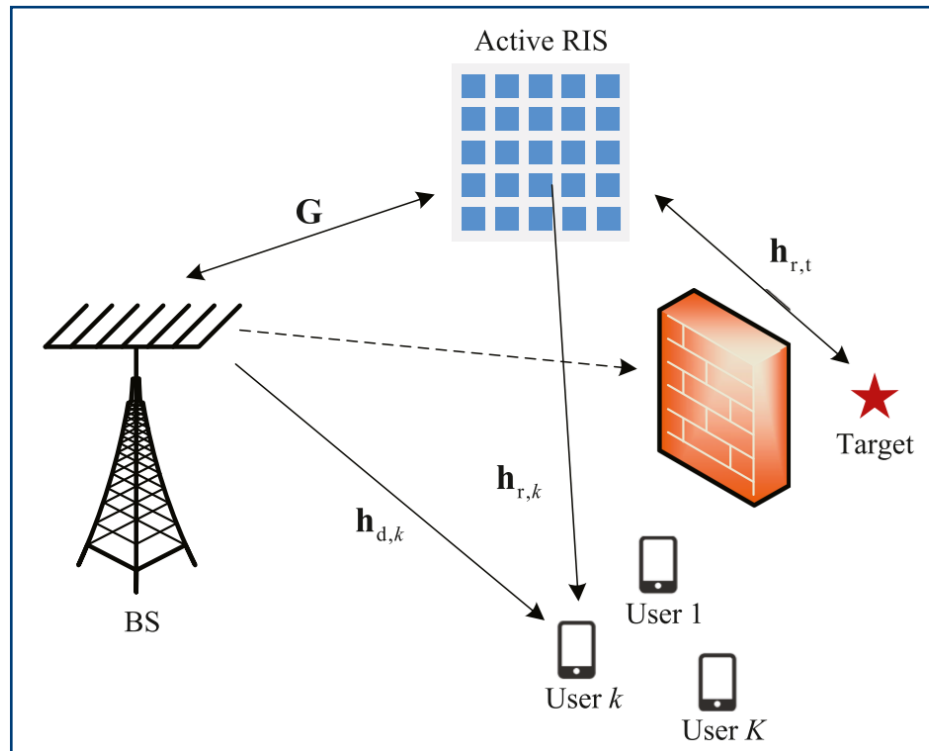


Fig. 6. An active RIS-assisted ISAC system [5].

Active RIS

- Multiplicative fading effect
- Reflection-type amplifiers
- Enhanced S&C performance
- Dynamic noise

- [4] Q. Zhu, M. Li, Rang Liu, and Q. Liu, "Cramer-Rao bound optimization for active RIS-empowered ISAC systems," *IEEE Trans. Wireless Commun.*, major revision.
- [5] Q. Zhu, M. Li, Rang Liu, and Q. Liu, "Joint transceiver beamforming and reflecting design for active RIS-aided ISAC systems," *IEEE Trans. Veh. Technol.*, vol. 72, no. 7, pp. 9636-9640, Jul. 2023.

Background of RIS-ISAC

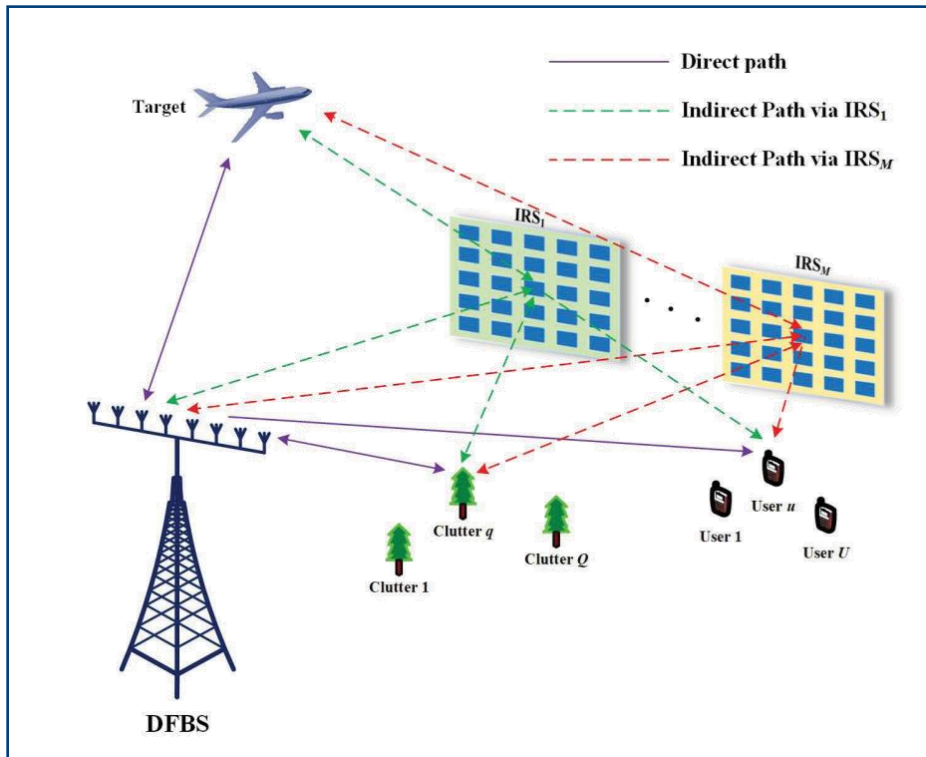


Fig. 7. A multi-RIS-aided ISAC system [6].

Multiple RISs

- Geographic diversity
- Hotspots/edge/blind areas
- High-dimensional optimization
- Deployment and control

[6] T. Wei, L. Wu, K. V. Mishra, and M. R. B. Shankar, “Multi-IRS-aided Doppler-tolerant wideband DFRC system,” *IEEE Trans. Commun.*, vol. 71, no. 11, pp. 6561-6577, Nov. 2023.

Background of RIS-ISAC

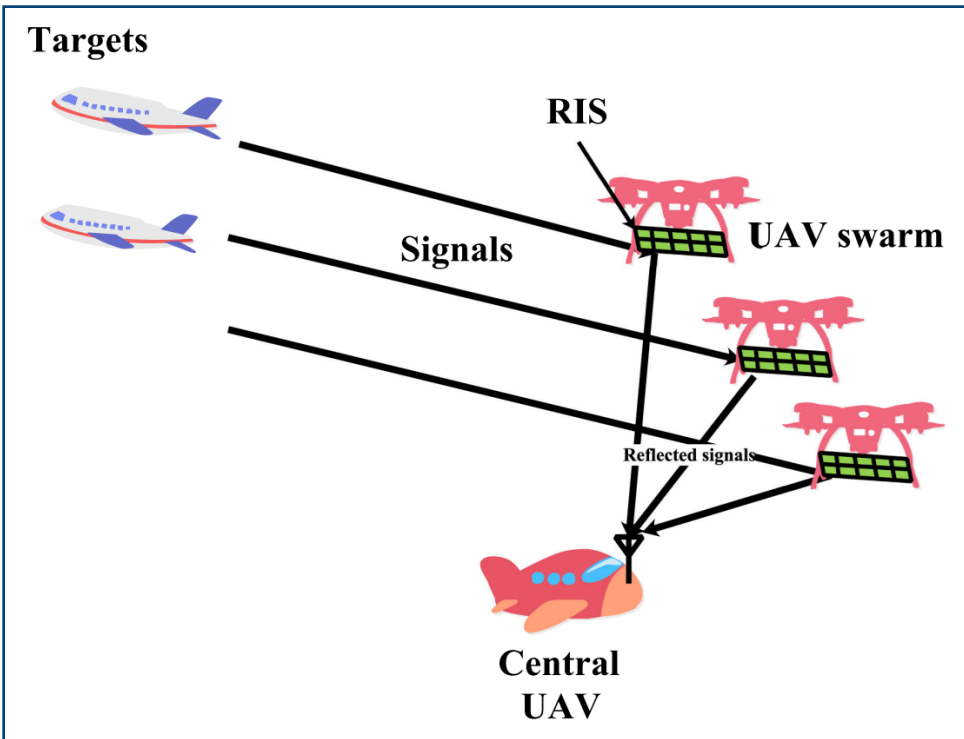


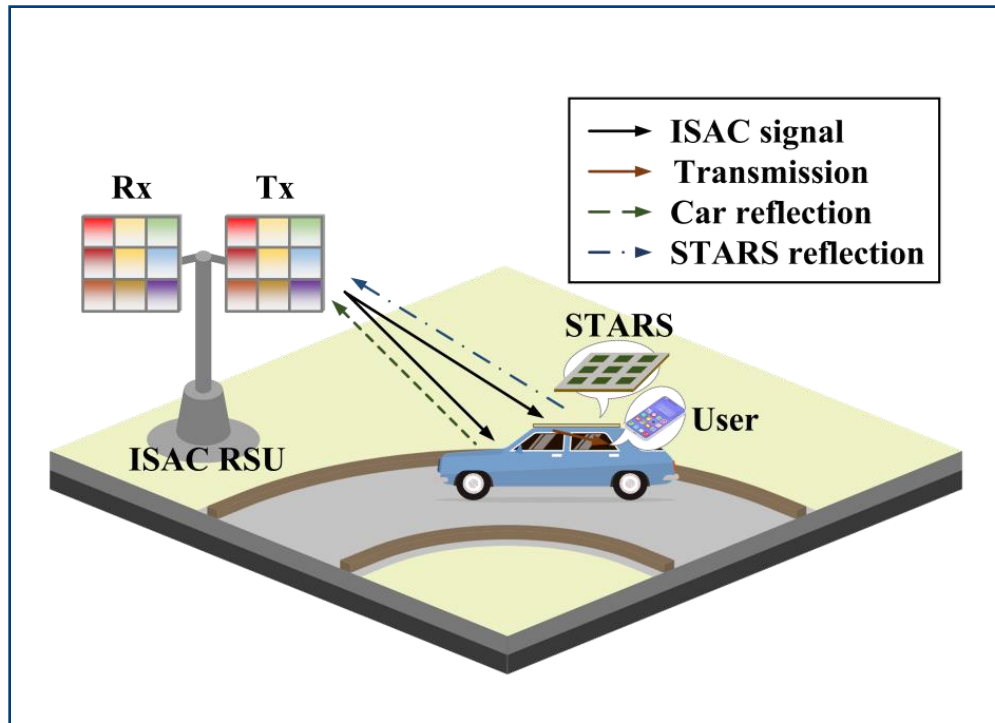
Fig. 8. An UAV-mounted RIS system [7].

UAV-mounted RIS

- High mobility and flexibility
- Wide coverage
- Joint UAV trajectory design

[7] P. Chen, Z. Chen, B. Zheng, and X. Wang, "Efficient DOA estimation method for reconfigurable intelligent surfaces aided UAV swarm," *IEEE Trans. Signal Process.*, vol. 70, pp. 743-755, 2022.

Background of RIS-ISAC

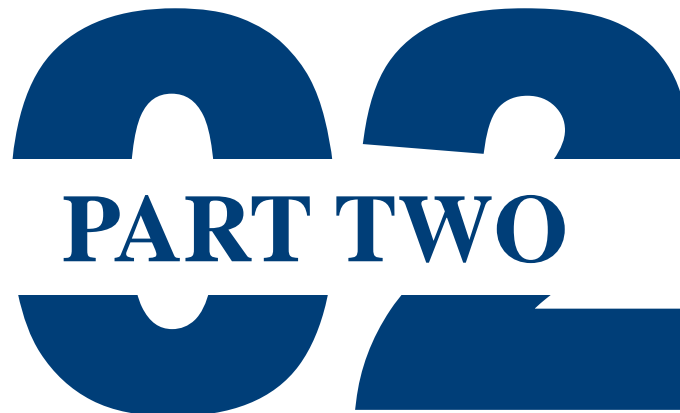


Target-mounted RIS

- Cooperative target
- Improve backscatter signals
- Control mechanisms

Fig. 9. The ISAC target-mounted STARS-assisted vehicular network [8].

[8] H. Zhang, Rang Liu, et al., "Joint sensing and communication optimization in target-mounted STARS-assisted vehicular networks: A MADRL approach," *IEEE Trans. Veh. Technol.*, to appear.

A large, dark blue graphic element shaped like four interlocking puzzle pieces, forming a U-shaped frame around the text.

PART TWO

General System Model

A thin, horizontal yellow line with small circular endpoints, extending from the left side of the slide towards the right.

System Model

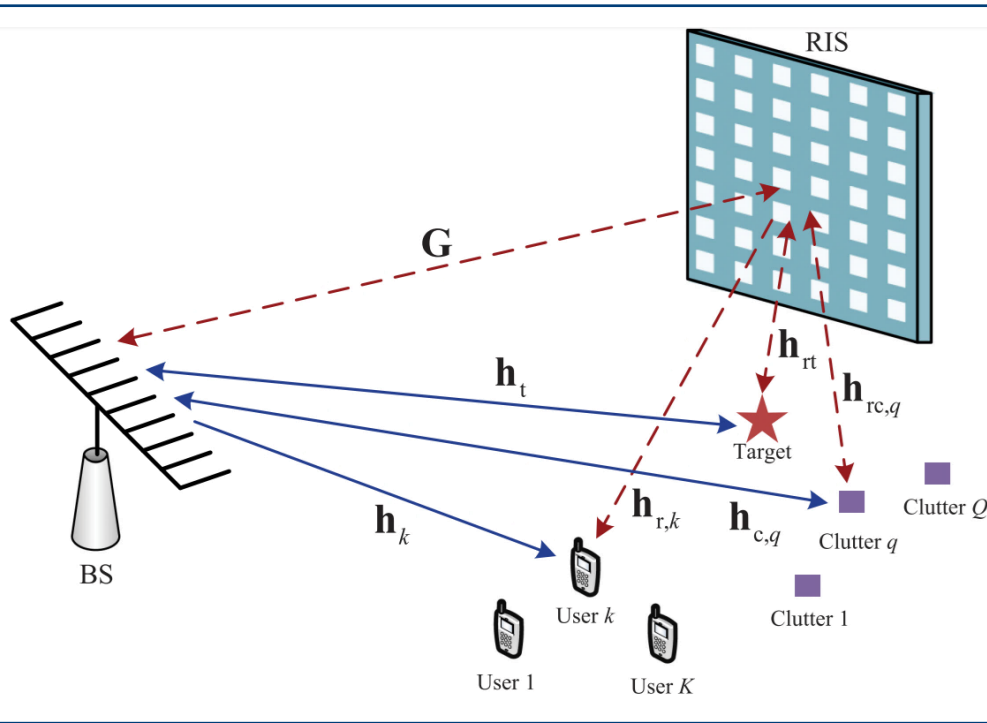


Fig. 10. A RIS-aided ISAC system.

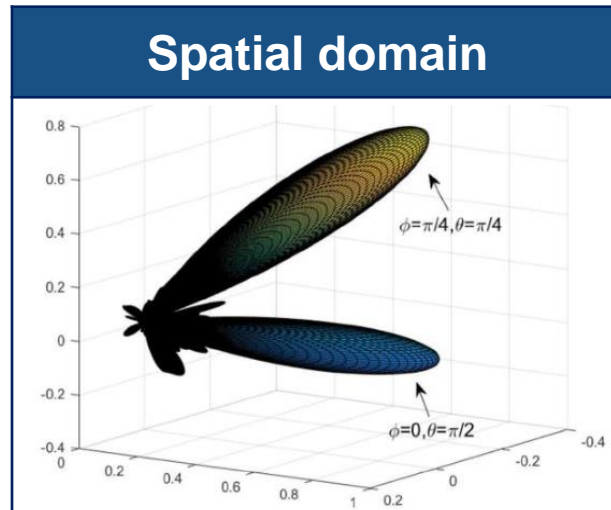
- **Motivations**
 - new optimization dimension
 - wide-coverage service
- **Contributions**
 - general system model
 - better S&C performance
- **Techniques**
 - space-time adaptive processing
 - symbol-level precoding

[9] Rang Liu, M. Li, Y. Liu, Q. Wu, and Q. Liu, “Joint transmit waveform and passive beamforming design for RIS-aided DFRC systems,” *IEEE J. Sel. Topics Signal Process.*, vol. 16, no. 5, pp. 995-1010, Aug. 2022.

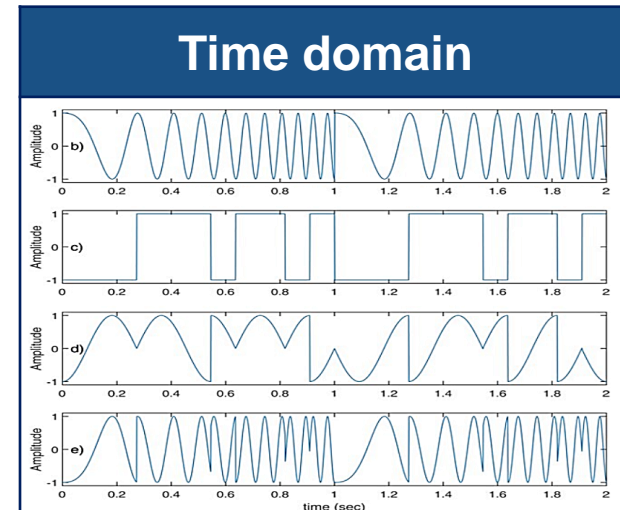
□ Performance metrics for sensing

- Target detection: identify the presence or absence of a target
 - **SNR/SINR/detection probability**
- Parameter estimation: estimate target azimuth angle/distance/velocity
 - **CRB**: the lower bound for any unbiased estimator
- General cases: favorable beampattern/waveform
 - beampattern, waveform similarity, mutual information, sidelobe level

□ Dual-functional waveform & beamforming design



VS



□ Performance metrics for communications

- reliability: SNR/SINR, rate/**sum-rate**, SER
- efficiency: power/spectral efficiency

□ Block-level precoding & symbol-level precoding

Linear BLP

- Transmit signal: $\mathbf{x}_m = \mathbf{W}\mathbf{s}_m$
 $\mathbf{X} = \mathbf{W}\mathbf{S}$
- $\mathbf{X} \triangleq [\mathbf{x}_1, \dots, \mathbf{x}_L] \quad \mathbf{S} \triangleq [\mathbf{s}_1, \dots, \mathbf{s}_L]$

- Receive signal:

$$y_{m,k} = \mathbf{h}_k^H \mathbf{W}\mathbf{s}_m + n_{m,k}$$

- Performance metric:

$$\text{SINR}_k = \frac{|\mathbf{h}_k^H \mathbf{w}_k|^2}{\sum_{j=1, j \neq k}^K |\mathbf{h}_k^H \mathbf{w}_j|^2 + \sigma_k^2}$$

- statistical information
- MUI suppression

VS

Non-Linear SLP

- Transmit signal:
 $\mathbf{s}_m \rightarrow \mathbf{x}_m$
- Receive signal:
 $r_{m,k} = \mathbf{h}_k^H \mathbf{x}_m + n_{m,k}$
- Performance metric:
safety margin
 - symbol-dependent
 - MUI exploitation

symbol inform. temporal DoFs

Radar Sensing Model

- The received signal at the BS:

$$\mathbf{r}[l] = \alpha_0 (\mathbf{h}_t + \mathbf{G}^H \Phi \mathbf{h}_{rt}) (\mathbf{h}_t^H + \mathbf{h}_{rt}^H \Phi \mathbf{G}) \mathbf{x}[l] e^{j2\pi(l-1)\nu_0} + \mathbf{c}[l] + \mathbf{z}[l]$$

target RCS 4 different paths Doppler frequency
 $\mathbf{H}_0(\phi)$

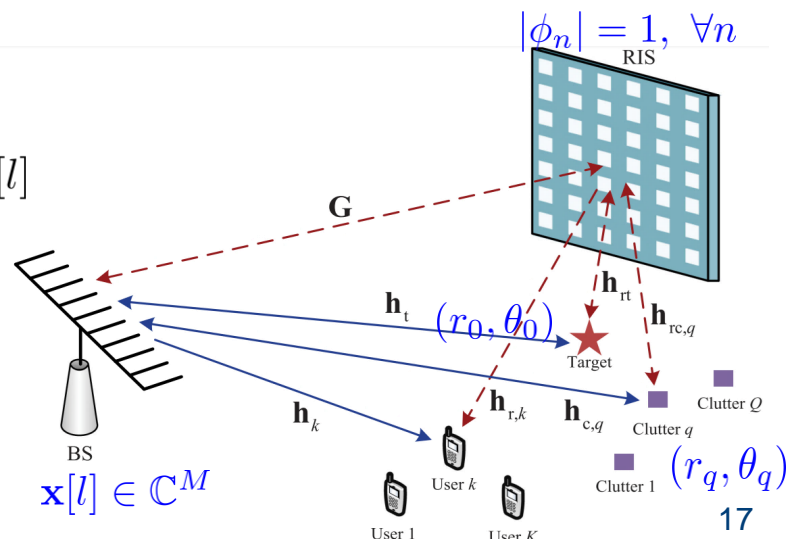
- Clutter returns:

$$\mathbf{c}[l] = \sum_{q=1}^Q \alpha_q (\mathbf{h}_{c,q} + \mathbf{G}^H \Phi \mathbf{h}_{rc,q}) (\mathbf{h}_{c,q}^H + \mathbf{h}_{rc,q}^H \Phi \mathbf{G}) \mathbf{x}[l - r_q] e^{j2\pi(l-1)\nu_q}$$

$\mathbf{H}_q(\phi)$ $\phi \triangleq [\phi_1, \dots, \phi_N]^T$

- The received signal in the l -th time slot:

$$\mathbf{r}[l] = \alpha_0 \mathbf{H}_0(\phi) \mathbf{x}[l] + \sum_{q=1}^Q \alpha_q \mathbf{H}_q(\phi) \mathbf{x}[l - r_q] + \mathbf{z}[l]$$



Sensing Performance Metrics

- The received signal during one CPI:

$$\mathbf{r} = \alpha_0 \tilde{\mathbf{H}}_0(\phi) \mathbf{x} + \sum_{q=1}^Q \alpha_q \tilde{\mathbf{H}}_q(\phi) \mathbf{x} + \mathbf{z}$$

$$\tilde{\mathbf{H}}_0(\phi) \triangleq \mathbf{I}_L \otimes \mathbf{H}_0(\phi), \quad \tilde{\mathbf{H}}_q(\phi) \triangleq [\mathbf{I}_L \otimes \mathbf{H}_q(\phi)] \mathbf{J}_{r_q}, \quad \mathbf{J}_{r_q}(i, j) = \begin{cases} 1, & i - j = Mr_q \\ 0, & \text{otherwise} \end{cases}$$

- The output after the linear space-time receive filter:

$$\mathbf{w}^H \mathbf{r} = \alpha_0 \mathbf{w}^H \tilde{\mathbf{H}}_0(\phi) \mathbf{x} + \mathbf{w}^H \sum_{q=1}^Q \alpha_q \tilde{\mathbf{H}}_q(\phi) \mathbf{x} + \mathbf{w}^H \mathbf{z}$$

- The radar output SINR:

$$\gamma_r = \frac{\varsigma_0^2 |\mathbf{w}^H \tilde{\mathbf{H}}_0(\phi) \mathbf{x}|^2}{\mathbf{w}^H \left[\sum_{q=1}^Q \varsigma_q^2 \tilde{\mathbf{H}}_q(\phi) \mathbf{x} \mathbf{x}^H \tilde{\mathbf{H}}_q^H(\phi) + \varsigma_z^2 \mathbf{I}_{ML} \right] \mathbf{w}}$$

- The constant-modulus waveform:

$$|x_i| = \sqrt{P/M}, \quad \forall i = 1, \dots, ML$$

Communication Model

- The communication symbols in the l -th time slot:

$$\mathbf{s}[l] \triangleq [s_1[l], \dots, s_K[l]]^T$$

- The received signal of the k -th user:

$$r_k[l] = (\mathbf{h}_k^H + \mathbf{h}_{r,k}^H \boldsymbol{\Phi} \mathbf{G}) \mathbf{x}[l] + n_k[l], \quad \forall l$$

- The received noise-free signal:

$$\overrightarrow{OD} = \tilde{r}_k[l] = (\mathbf{h}_k^H + \mathbf{h}_{r,k}^H \boldsymbol{\Phi} \mathbf{G}) \mathbf{x}[l]$$

$$\tilde{r}_k[l] = [\mathbf{e}_l^T \otimes (\mathbf{h}_k^H + \boldsymbol{\phi}^T \text{diag}\{\mathbf{h}_{r,k}^H\} \mathbf{G})] \mathbf{x}$$

- The desired symbol with the required SNR:

$$\overrightarrow{OA} = \sigma_k \sqrt{\Gamma_k} s_k[l]$$

- The multiuser interference:

$$\overrightarrow{OD} - \overrightarrow{OA} = (\mathbf{h}_k^H + \mathbf{h}_{r,k}^H \boldsymbol{\Phi} \mathbf{G}) \mathbf{x}[l] - \sigma_k \sqrt{\Gamma_k} s_k[l]$$

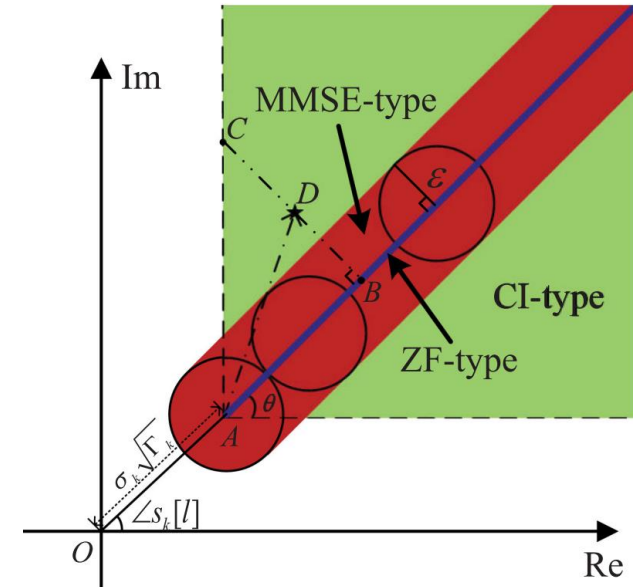


Fig. 11. Illustration of handling MUI.

- ZF-type communication metric:

$$(\mathbf{h}_k^H + \mathbf{h}_{r,k}^H \Phi \mathbf{G}) \mathbf{x}[l] = \sigma_k \sqrt{\Gamma_k} s_k[l]$$

↓

$$(\mathbf{h}_k^H + \mathbf{h}_{r,k}^H \Phi \mathbf{G}) \mathbf{x}[l] = \alpha_{k,l} \sigma_k \sqrt{\Gamma_k} s_k[l], \quad \alpha_{k,l} \geq 1, \quad \forall k, l$$

scaling factor

- MMSE-type communication metric:

$$|(\mathbf{h}_k^H + \mathbf{h}_{r,k}^H \Phi \mathbf{G}) \mathbf{x}[l] - \alpha_{k,l} \sigma_k \sqrt{\Gamma_k} s_k[l]|^2 \leq \epsilon, \quad \alpha_{k,l} \geq 1, \quad \forall k, l$$

- CI-type communication metric:

$$\begin{aligned} & \Re\{(\mathbf{h}_k^H + \mathbf{h}_{r,k}^H \Phi \mathbf{G}) \mathbf{x}[l] e^{-j\angle s_k[l]} - \sigma_k \sqrt{\Gamma_k}\} \sin \theta \\ & - |\Im\{(\mathbf{h}_k^H + \mathbf{h}_{r,k}^H \Phi \mathbf{G}) \mathbf{x}[l] e^{-j\angle s_k[l]}\}| \cos \theta \geq 0, \quad \forall k, l \end{aligned}$$

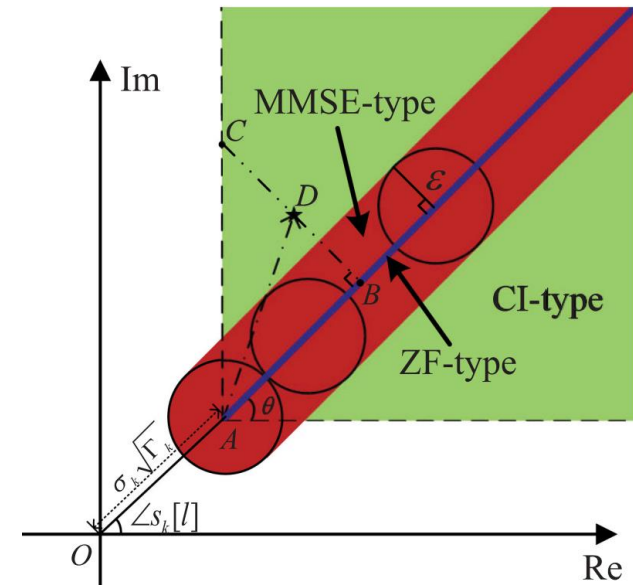
- Reformulated as

$$[\mathbf{h}_{k,l}^H + (\mathbf{e}_l^T \otimes \boldsymbol{\phi}^T) \mathbf{G}_k] \mathbf{x} = \alpha_{k,l} \gamma_{k,l}^{\text{ZF}}, \quad \alpha_{k,l} \geq 1, \quad \forall k, l$$

$$|[\mathbf{h}_{k,l}^H + (\mathbf{e}_l^T \otimes \boldsymbol{\phi}^T) \mathbf{G}_k] \mathbf{x} - \alpha_{k,l} \gamma_{k,l}^{\text{ZF}}|^2 \leq \epsilon, \quad \alpha_{k,l} \geq 1, \quad \forall k, l$$

$$\Re\{\gamma_{k,l}^{\text{CI}} [\mathbf{h}_{k,l}^H + (\mathbf{e}_l^T \otimes \boldsymbol{\phi}^T) \mathbf{G}_k] \mathbf{x}\} \geq 1, \quad \forall k, l$$

Different strategies of handling MUI



|| Problem Formulation

$$\begin{aligned}
 & \max_{\mathbf{x}, \boldsymbol{\alpha}, \mathbf{w}, \boldsymbol{\phi}} \frac{\varsigma_0^2 |\mathbf{w}^H \tilde{\mathbf{H}}_0(\boldsymbol{\phi}) \mathbf{x}|^2}{\mathbf{w}^H \left[\sum_{q=1}^Q \varsigma_q^2 \tilde{\mathbf{H}}_q(\boldsymbol{\phi}) \mathbf{x} \mathbf{x}^H \tilde{\mathbf{H}}_q^H(\boldsymbol{\phi}) + \varsigma_z^2 \mathbf{I}_{ML} \right] \mathbf{w}} \\
 & \text{s.t. communication QoS constraints} \\
 & \quad |x_i| = \sqrt{P/M}, \quad \forall i \\
 & \quad |\phi_n| = 1, \quad \forall n
 \end{aligned}$$

- The optimal solution to the receive filter:

$$\mathbf{w}^* = \frac{\left[\sum_{q=1}^Q \varsigma_q^2 \tilde{\mathbf{H}}_q(\boldsymbol{\phi}) \mathbf{x} \mathbf{x}^H \tilde{\mathbf{H}}_q^H(\boldsymbol{\phi}) + \varsigma_z^2 \mathbf{I} \right]^{-1} \tilde{\mathbf{H}}_0(\boldsymbol{\phi}) \mathbf{x}}{\mathbf{x}^H \tilde{\mathbf{H}}_0^H(\boldsymbol{\phi}) \left[\sum_{q=1}^Q \varsigma_q^2 \tilde{\mathbf{H}}_q(\boldsymbol{\phi}) \mathbf{x} \mathbf{x}^H \tilde{\mathbf{H}}_q^H(\boldsymbol{\phi}) + \varsigma_z^2 \mathbf{I} \right]^{-1} \tilde{\mathbf{H}}_0(\boldsymbol{\phi}) \mathbf{x}}$$

- The optimization problem is transformed into:

$$\begin{aligned}
 & \min_{\mathbf{x}, \boldsymbol{\alpha}, \boldsymbol{\phi}} -\mathbf{x}^H \tilde{\mathbf{H}}_0^H(\boldsymbol{\phi}) \left[\sum_{q=1}^Q \varsigma_q^2 \tilde{\mathbf{H}}_q(\boldsymbol{\phi}) \mathbf{x} \mathbf{x}^H \tilde{\mathbf{H}}_q^H(\boldsymbol{\phi}) + \varsigma_z^2 \mathbf{I} \right]^{-1} \tilde{\mathbf{H}}_0(\boldsymbol{\phi}) \mathbf{x} \\
 & \text{s.t. communication QoS constraints} \\
 & \quad |x_i| = \sqrt{P/M}, \quad \forall i \\
 & \quad |\phi_n| = 1, \quad \forall n
 \end{aligned}$$



PART THREE

Joint Designs for RIS-ISAC



Joint Transmit Waveform and Beamforming Design

A. ADMM-based transformation

$$\min_{\mathbf{x}, \boldsymbol{\alpha}, \mathbf{y}, \boldsymbol{\varphi}, \boldsymbol{\phi}} f_1(\mathbf{x}, \boldsymbol{\phi}) \triangleq -\mathbf{x}^H \tilde{\mathbf{H}}_0^H(\boldsymbol{\phi}) \left[\sum_{q=1}^Q \varsigma_q^2 \tilde{\mathbf{H}}_q(\boldsymbol{\phi}) \mathbf{x} \mathbf{x}^H \tilde{\mathbf{H}}_q^H(\boldsymbol{\phi}) + \varsigma_z^2 \mathbf{I} \right]^{-1} \tilde{\mathbf{H}}_0(\boldsymbol{\phi}) \mathbf{x}$$

s.t. communication QoS constraints

$$|x_i| \leq \sqrt{P/M}, \quad \forall i$$

$$|\phi_n| \leq 1, \quad \forall n$$

$$|y_i| = \sqrt{P/M}, \quad \forall i$$

$$|\varphi_n| = 1, \quad \forall n$$

indicator function
 $\mathbb{I}(\mathbf{x}, \boldsymbol{\alpha}, \mathbf{y}, \boldsymbol{\phi}, \boldsymbol{\varphi})$

$$\mathbf{y} = \mathbf{x}$$

$$\boldsymbol{\varphi} = \boldsymbol{\phi}$$

auxiliary variables



$$\begin{aligned} & \min_{\mathbf{x}, \boldsymbol{\alpha}, \mathbf{y}, \boldsymbol{\varphi}, \boldsymbol{\phi}} f_1(\mathbf{x}, \boldsymbol{\phi}) + \mathbb{I}(\mathbf{x}, \boldsymbol{\alpha}, \mathbf{y}, \boldsymbol{\phi}, \boldsymbol{\varphi}) \\ & \text{s.t. } \mathbf{y} = \mathbf{x} \\ & \quad \boldsymbol{\varphi} = \boldsymbol{\phi} \end{aligned}$$



- The augmented Lagrangian function:

$$\begin{aligned} \mathcal{L}(\mathbf{x}, \boldsymbol{\alpha}, \mathbf{y}, \boldsymbol{\phi}, \boldsymbol{\varphi}, \boldsymbol{\mu}_1, \boldsymbol{\mu}_2) & \triangleq f_1(\mathbf{x}, \boldsymbol{\phi}) + \mathbb{I}(\mathbf{x}, \boldsymbol{\alpha}, \mathbf{y}, \boldsymbol{\phi}, \boldsymbol{\varphi}) \\ & + \frac{\rho}{2} \left\| \mathbf{x} - \mathbf{y} + \frac{\boldsymbol{\mu}_1}{\rho} \right\|^2 + \frac{\rho}{2} \left\| \boldsymbol{\phi} - \boldsymbol{\varphi} + \frac{\boldsymbol{\mu}_2}{\rho} \right\|^2 \end{aligned}$$

B. MM-based transformation

- A surrogate function constructed by using the first-order Taylor expansion:

$$\mathbf{s}^H \mathbf{M}^{-1} \mathbf{s} \geq 2\Re\{\mathbf{s}_t^H \mathbf{M}_t^{-1} \mathbf{s}\} - \text{Tr}\{\mathbf{M}_t^{-1} \mathbf{s}_t \mathbf{s}_t^H \mathbf{M}_t^{-1} \mathbf{M}\} + c$$



$$f_1(\mathbf{x}, \boldsymbol{\phi}) \leq \text{Tr}\left\{\mathbf{M}_t^{-1} \mathbf{s}_t \mathbf{s}_t^H \mathbf{M}_t^{-1} \left[\sum_{q=1}^Q \varsigma_q^2 \tilde{\mathbf{H}}_q(\boldsymbol{\phi}) \mathbf{x} \mathbf{x}^H \tilde{\mathbf{H}}_q^H(\boldsymbol{\phi}) \right] \right\} - 2\Re\{\mathbf{s}_t^H \mathbf{M}_t^{-1} \tilde{\mathbf{H}}_0(\boldsymbol{\phi}) \mathbf{x}\} + c_1$$



- The surrogate AL function:

$$\begin{aligned} \mathcal{L}(\mathbf{x}, \boldsymbol{\alpha}, \mathbf{y}, \boldsymbol{\phi}, \boldsymbol{\varphi}, \boldsymbol{\mu}_1, \boldsymbol{\mu}_2) \leq & \text{Tr}\left\{\mathbf{M}_t^{-1} \mathbf{s}_t \mathbf{s}_t^H \mathbf{M}_t^{-1} \left[\sum_{q=1}^Q \varsigma_q^2 \tilde{\mathbf{H}}_q(\boldsymbol{\phi}) \mathbf{x} \mathbf{x}^H \tilde{\mathbf{H}}_q^H(\boldsymbol{\phi}) \right] \right\} \\ & - 2\Re\{\mathbf{s}_t^H \mathbf{M}_t^{-1} \tilde{\mathbf{H}}_0(\boldsymbol{\phi}) \mathbf{x}\} + c_1 + \mathbb{I}(\mathbf{x}, \boldsymbol{\alpha}, \mathbf{y}, \boldsymbol{\phi}, \boldsymbol{\varphi}) \\ & + \frac{\rho}{2} \left\| \mathbf{x} - \mathbf{y} + \frac{\boldsymbol{\mu}_1}{\rho} \right\|^2 + \frac{\rho}{2} \left\| \boldsymbol{\phi} - \boldsymbol{\varphi} + \frac{\boldsymbol{\mu}_2}{\rho} \right\|^2 \end{aligned}$$



Block update

C. Update \mathbf{x} and α

$$\begin{aligned}
 \min_{\mathbf{x}, \alpha} \quad & \mathbf{x}^H \mathbf{D}_t \mathbf{x} + \Re\{\mathbf{d}_t^H \mathbf{x}\} \\
 \text{s.t.} \quad & \tilde{\mathbf{h}}_{k,l}^H \mathbf{x} = \alpha_{k,l} \gamma_{k,l}^{\text{ZF}}, \quad \alpha_{k,l} \geq 1, \quad \forall k, l \\
 & \text{or } |\tilde{\mathbf{h}}_{k,l}^H \mathbf{x} - \alpha_{k,l} \gamma_{k,l}^{\text{ZF}}|^2 \leq \epsilon, \quad \alpha_{k,l} \geq 1, \quad \forall k, l \\
 & \text{or } \Re\{\gamma_{k,l}^{\text{CI}} \tilde{\mathbf{h}}_{k,l}^H \mathbf{x}\} \geq 1, \quad \forall k, l \\
 & |x_i| \leq \sqrt{P/M}, \quad \forall i
 \end{aligned}
 \tag{Convex problem}$$

D. Update \mathbf{y}

$$\begin{aligned}
 \min_{\mathbf{y}} \quad & \left\| \mathbf{x}_t - \mathbf{y} + \frac{\boldsymbol{\mu}_1}{\rho} \right\|^2 \\
 \text{s.t.} \quad & |y_i| = \sqrt{P/M}, \quad \forall i
 \end{aligned}
 \quad \Rightarrow \quad \mathbf{y}^* = \sqrt{P/M} e^{j\angle(\rho \mathbf{x}_t + \boldsymbol{\mu}_1)}$$

E. Update $\boldsymbol{\phi}$

$$\begin{aligned}
 \min_{\boldsymbol{\phi}} \quad & f_2(\boldsymbol{\phi}) = \boldsymbol{\phi}^H \mathbf{F}_t \boldsymbol{\phi} + \Re\{\boldsymbol{\phi}^H \mathbf{f}_t\} + \mathbf{v}^H \mathbf{F}_{v,t} \mathbf{v} + \Re\{\mathbf{v}^H \mathbf{f}_{v,t}\} \\
 & + \Re\{\mathbf{v}^H \mathbf{L}_t \boldsymbol{\phi}\} + c_2 + \frac{\rho}{2} \left\| \boldsymbol{\phi} - \boldsymbol{\varphi}_t + \frac{\boldsymbol{\mu}_2}{\rho} \right\|^2
 \end{aligned}$$

s.t. communication QoS constraints

$$|\phi_n| \leq 1, \quad \forall n$$

$$\begin{aligned}
 \mathbf{v} &\triangleq \text{vec}\{\boldsymbol{\phi} \boldsymbol{\phi}^T\} \\
 &= \boldsymbol{\phi} \otimes \boldsymbol{\phi}
 \end{aligned}$$

- Construct a tractable surrogate function

$$\begin{aligned}
 f_2(\phi) &\leq \phi^H \mathbf{F}_t \phi + \Re\{\phi^H \mathbf{f}_t\} + \frac{\lambda_2}{2} \phi^H \phi + \Re\{\phi^H \mathbf{U} \bar{\mathbf{f}}_{v,t}\} + c_3 \\
 &\quad + c_4 + \frac{\lambda_3}{2} \phi^H \phi + \Re\{\phi^H \mathbf{U} \bar{\ell}_t\} + c_5 + c_2 + \frac{\rho}{2} \left\| \phi - \varphi_t + \frac{\mu_2}{\rho} \right\|^2 \\
 &= \phi^H \tilde{\mathbf{F}}_t \phi + \Re\{\phi^H \tilde{\mathbf{f}}_t\} + c_6
 \end{aligned}$$

- Solve for ϕ

$$\begin{aligned}
 \min_{\phi} \quad & \phi^H \tilde{\mathbf{F}}_t \phi + \Re\{\phi^H \tilde{\mathbf{f}}_t\} \\
 \text{s.t.} \quad & \mathbf{h}_{k,l}^H \mathbf{x} + \tilde{\mathbf{g}}_{k,l}^T \phi = \alpha_{k,l} \gamma_{k,l}^{\text{ZF}}, \quad \alpha_{k,l} \geq 1, \quad \forall k, l \\
 & \text{or } \left| \mathbf{h}_{k,l}^H \mathbf{x} + \tilde{\mathbf{g}}_{k,l}^T \phi - \alpha_{k,l} \gamma_{k,l}^{\text{ZF}} \right|^2 \leq \epsilon, \quad \alpha_{k,l} \geq 1, \quad \forall k, l \\
 & \text{or } \Re\{\gamma_{k,l}^{\text{CI}} (\mathbf{h}_{k,l}^H \mathbf{x} + \tilde{\mathbf{g}}_{k,l}^T \phi)\} \geq 1, \quad \forall k, l \\
 & |\phi_n| \leq 1, \quad \forall n
 \end{aligned}$$

Convex problem

F. Update φ $\varphi^* = e^{j\angle(\rho\phi_t + \mu_2)}$

G. Update the dual variables: $\mu_1 := \mu_1 + \rho(\mathbf{x}_t - \mathbf{y}_t)$
 $\mu_2 := \mu_2 + \rho(\phi_t - \varphi_t)$

H. Initialization

- The optimization problem of initializing Φ

$$\begin{aligned} \max_{\phi} \quad & \| \mathbf{h}_t^H + \mathbf{h}_{rt}^H \Phi \mathbf{G} \|^2 + \sum_{k=1}^K \| \mathbf{h}_k^H + \mathbf{h}_{r,k}^H \Phi \mathbf{G} \|^2 - \sum_{q=1}^Q \| \mathbf{h}_{c,q}^H + \mathbf{h}_{rc,q}^H \Phi \mathbf{G} \|^2 \\ \text{s.t.} \quad & |\phi_n| = 1, \quad \forall n \end{aligned}$$

- solved by manifold optimization algorithm, etc.

- The optimization problem of initializing \mathbf{x}

$$\begin{aligned} \max_{\mathbf{x}} \quad & \min_{k,l} \alpha_{k,l} \\ \text{s.t.} \quad & [\mathbf{h}_{k,l}^H + (\mathbf{e}_l^T \otimes \phi^T) \mathbf{G}_k] \mathbf{x} = \alpha_{k,l} \gamma_{k,l}^{\text{ZF}}, \quad \forall k, l, \\ & \text{or } |[\mathbf{h}_{k,l}^H + (\mathbf{e}_l^T \otimes \phi^T) \mathbf{G}_k] \mathbf{x} - \alpha_{k,l} \gamma_{k,l}^{\text{ZF}}|^2 \leq \epsilon, \quad \forall k, l \\ & |x_i| \leq \sqrt{P/M}, \quad \forall i \end{aligned}$$

Convex problems

$$\begin{aligned} \max_{\mathbf{x}} \quad & \min_{k,l} \Re \{ \tilde{\mathbf{h}}_{k,l}^H \mathbf{x} \} \\ \text{s.t.} \quad & |x_i| \leq \sqrt{P/M}, \quad \forall i \end{aligned}$$

Simulation Results

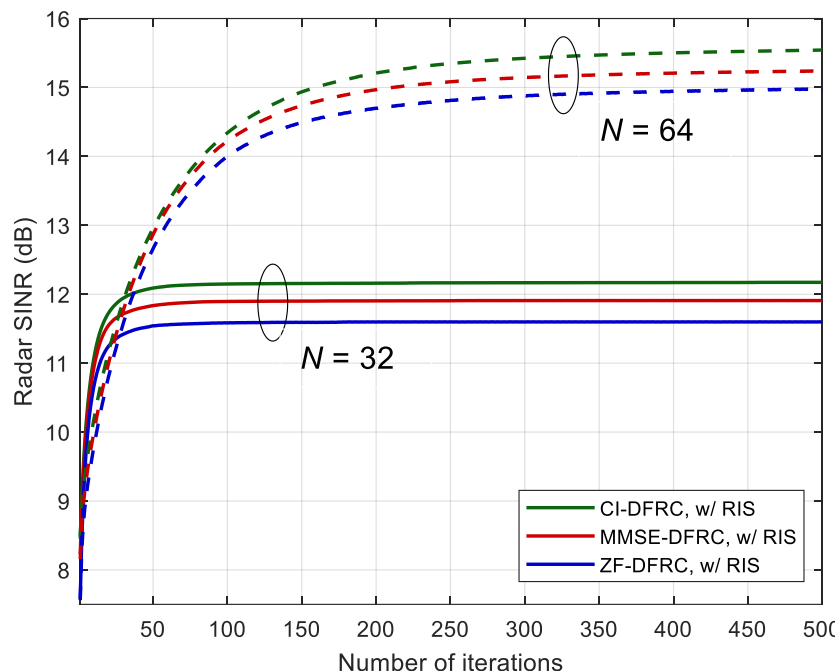


Fig. 12. Convergence illustration.

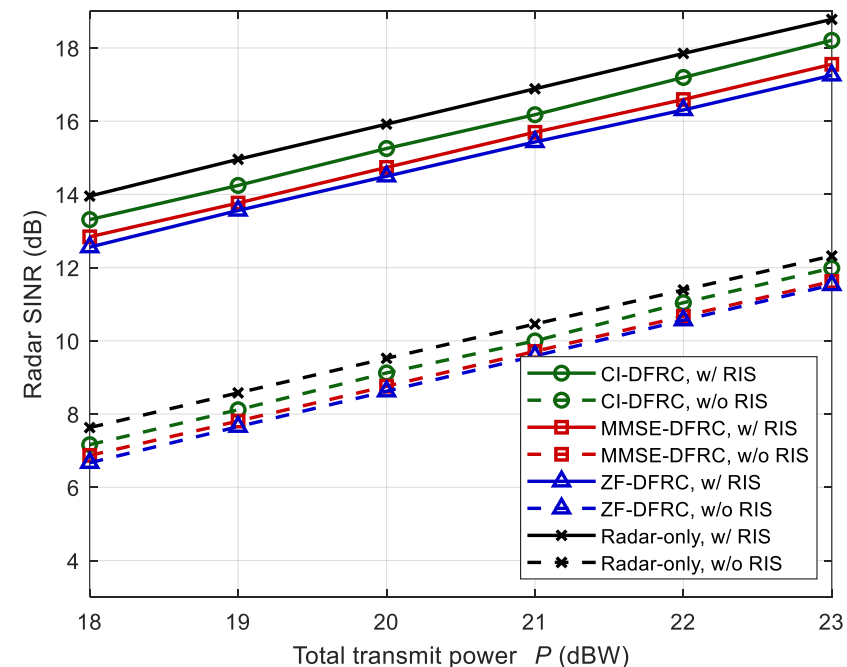


Fig. 13. Radar SINR versus total transmit power.

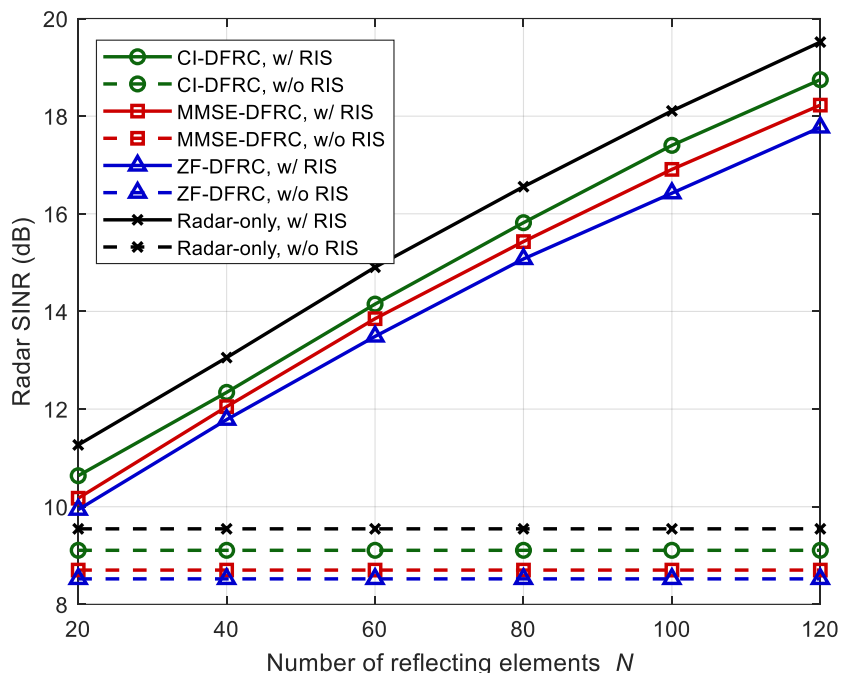


Fig. 14. Radar SINR versus N .

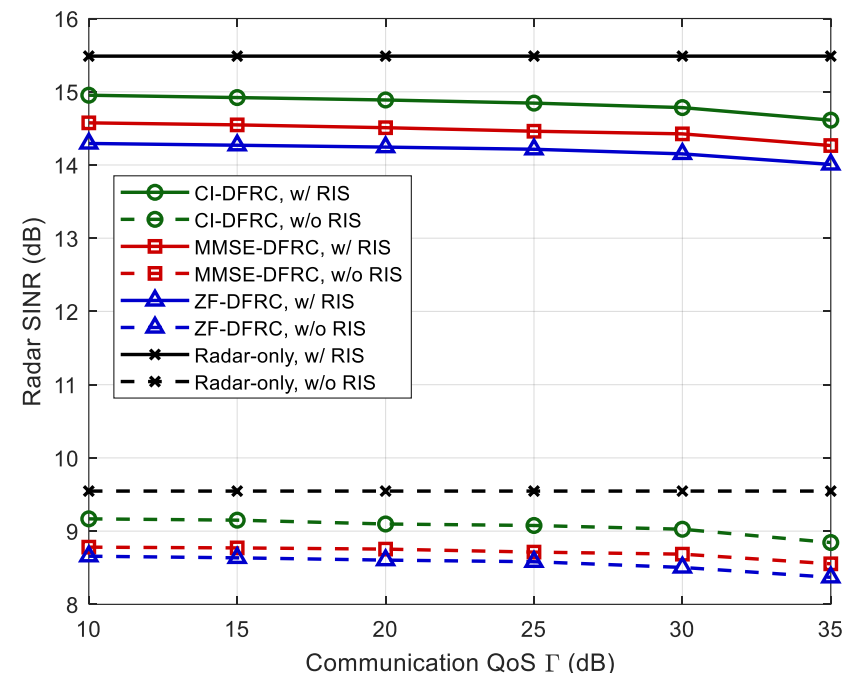


Fig. 15. Radar SINR versus communication QoS.

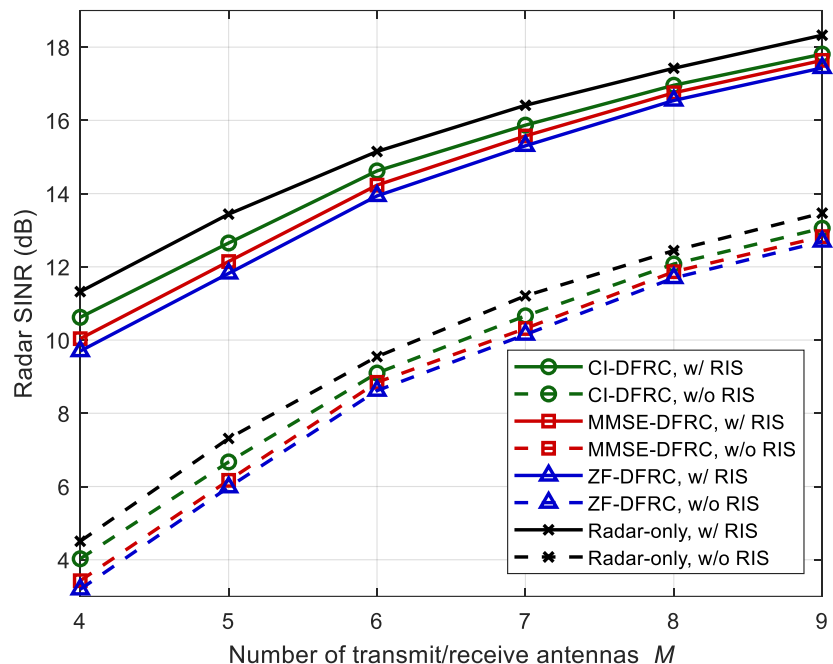


Fig. 16. Radar SINR versus M .

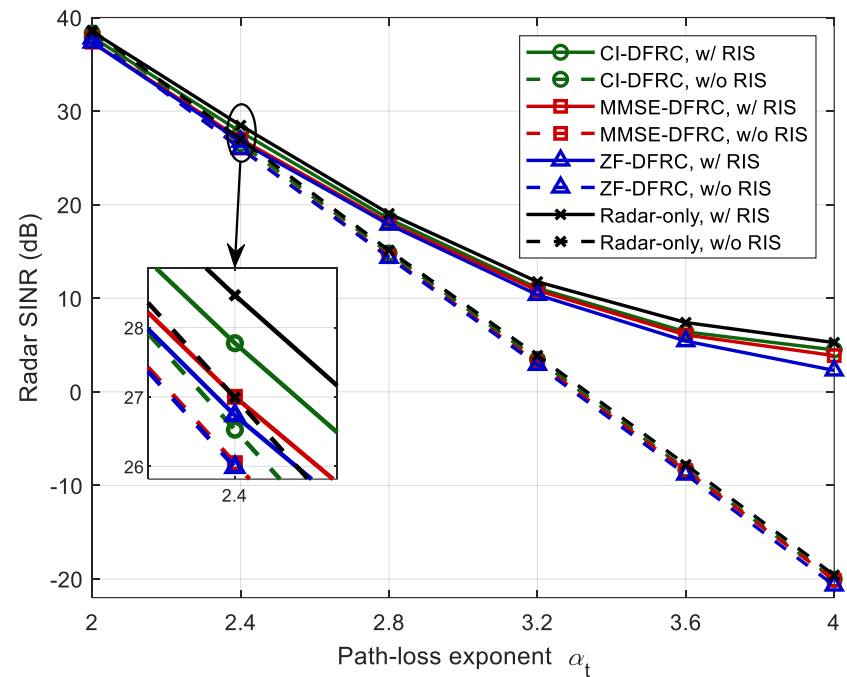


Fig. 17. Radar SINR versus path-loss exponent.

Joint Beamforming Designs for RIS-ISAC Systems

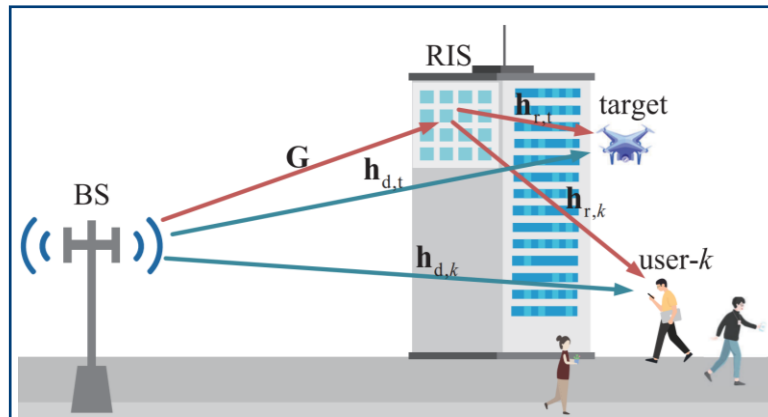


Fig. 18. An RIS-assisted ISAC system.

Contributions

- joint beamforming designs
- detection & estimation
- sum-rate maximization

- Transmitted dual-functional signal: $\mathbf{x}[l] = \mathbf{W}_c \mathbf{s}_c[l] + \mathbf{W}_r \mathbf{s}_r[l] = \mathbf{W}\mathbf{s}[l]$
- The received signal at the k -th user: $y_k[l] = (\mathbf{h}_{d,k}^T + \mathbf{h}_{r,k}^T \Phi \mathbf{G}) \mathbf{x}[l] + n_k[l]$
- The received echo signals at the BS:

$$\mathbf{y}_r[l] = \alpha_t (\mathbf{h}_{d,t} + \mathbf{G}^T \Phi \mathbf{h}_{r,t}) (\mathbf{h}_{d,t}^T + \mathbf{h}_{r,t}^T \Phi \mathbf{G}) \mathbf{W}\mathbf{s}[l] + \mathbf{n}_r[l]$$

- Matched-filtering: $\tilde{\mathbf{Y}}_r = \alpha_t \mathbf{H}_t(\phi) \mathbf{W} \mathbf{S}^H + \mathbf{N}_r \mathbf{S}^H$

Target detection

- Vectorized output: $\tilde{\mathbf{y}}_r = \alpha_t (\mathbf{S} \mathbf{S}^H \otimes \mathbf{H}_t(\phi)) \mathbf{w} + \tilde{\mathbf{n}}_r$

- Receive beamformer: $\mathbf{u}^H \tilde{\mathbf{y}}_r = \alpha_t \mathbf{u}^H (\mathbf{S} \mathbf{S}^H \otimes \mathbf{H}_t(\phi)) \mathbf{w} + \mathbf{u}^H \tilde{\mathbf{n}}_r$

- Detection probability: $P_D \propto \eta_1 / \eta_0 = \frac{\sigma_t^2 \mathbb{E}\{| \mathbf{u}^H (\mathbf{S} \mathbf{S}^H \otimes \mathbf{H}_t(\phi)) \mathbf{w} |^2\}}{L \sigma_r^2 \mathbf{u}^H \mathbf{u}} + 1$

$$\mathbb{E}\{f(x)\} \geq f(\mathbb{E}\{x\}) \quad \downarrow \quad \mathbb{E}\{\mathbf{S} \mathbf{S}^H\} = L \mathbf{I}_{K+M}$$

- Worst-case radar SNR: $\text{SNR}_t \geq \frac{L \sigma_t^2 |\mathbf{u}^H (\mathbf{I}_{K+M} \otimes \mathbf{H}_t(\phi)) \mathbf{w}|^2}{\sigma_r^2 \mathbf{u}^H \mathbf{u}}$

- SNR-constrained joint design:

$$\begin{aligned} & \max_{\mathbf{W}, \mathbf{u}, \phi} \quad \sum_{k=1}^K \log_2 (1 + \text{SINR}_k) \\ \text{s.t.} \quad & \frac{L \sigma_t^2 |\mathbf{u}^H (\mathbf{I}_{K+M} \otimes \mathbf{H}_t(\phi)) \mathbf{w}|^2}{\sigma_r^2 \mathbf{u}^H \mathbf{u}} \geq \Gamma_t \\ & \|\mathbf{W}\|_F^2 \leq P_t \\ & |\phi_n| = 1, \quad \forall n \end{aligned}$$

- Unknown target parameter: $\xi \triangleq [\boldsymbol{\theta}^T, \boldsymbol{\alpha}^T]^T$

$$\boldsymbol{\theta} \triangleq [\theta_1, \theta_2]^T \quad \boldsymbol{\alpha} \triangleq [\Re\{\alpha_t\}, \Im\{\alpha_t\}]^T$$

DoA Estimation

- Vectorized received signal: $\mathbf{y}_r = \alpha_t \text{vec}\{\mathbf{H}_t(\phi) \mathbf{W} \mathbf{S}\} + \mathbf{n}_r$

- Fisher information matrix: $\mathbf{F}_{IM}(i, j) = \frac{2}{\sigma_r^2} \Re \left\{ \frac{\partial^H \boldsymbol{\eta}}{\partial \xi_i} \frac{\partial \boldsymbol{\eta}}{\partial \xi_j} \right\}$

$$\mathbf{F}_{IM} = \begin{bmatrix} \mathbf{F}_{\boldsymbol{\theta}\boldsymbol{\theta}^T} & \mathbf{F}_{\boldsymbol{\theta}\boldsymbol{\alpha}^T} \\ \mathbf{F}_{\boldsymbol{\theta}\boldsymbol{\alpha}^T}^T & \mathbf{F}_{\boldsymbol{\alpha}\boldsymbol{\alpha}^T} \end{bmatrix} = \begin{bmatrix} \mathbf{C}_{\boldsymbol{\theta}\boldsymbol{\theta}^T} & \mathbf{C}_{\boldsymbol{\theta}\boldsymbol{\alpha}^T} \\ \mathbf{C}_{\boldsymbol{\alpha}\boldsymbol{\theta}^T} & \mathbf{C}_{\boldsymbol{\alpha}\boldsymbol{\alpha}^T} \end{bmatrix}^{-1} = \mathbf{C}^{-1}$$

- The CRB for estimating DoAs:

$$\text{CRB}_{\theta_1} + \text{CRB}_{\theta_2} = \text{Tr}\{\mathbf{C}_{\boldsymbol{\theta}\boldsymbol{\theta}^T}\} = \text{Tr}\{(\mathbf{F}_{\boldsymbol{\theta}\boldsymbol{\theta}^T} - \mathbf{F}_{\boldsymbol{\theta}\boldsymbol{\alpha}^T} \mathbf{F}_{\boldsymbol{\alpha}\boldsymbol{\alpha}^T}^{-1} \mathbf{F}_{\boldsymbol{\theta}\boldsymbol{\alpha}^T}^T)^{-1}\}$$

- CRB-constrained joint design:

$$\begin{aligned} \max_{\mathbf{W}, \phi} \quad & \sum_{k=1}^K \log_2(1 + \text{SINR}_k) \\ \text{s.t.} \quad & \text{Tr}\{(\mathbf{F}_{\boldsymbol{\theta}\boldsymbol{\theta}^T} - \mathbf{F}_{\boldsymbol{\theta}\boldsymbol{\alpha}^T} \mathbf{F}_{\boldsymbol{\alpha}\boldsymbol{\alpha}^T}^{-1} \mathbf{F}_{\boldsymbol{\theta}\boldsymbol{\alpha}^T}^T)^{-1}\} \leq \varepsilon \\ & \|\mathbf{W}\|_F^2 \leq P_t \\ & |\phi_n| = 1, \quad \forall n \end{aligned}$$

|| Simulation Results

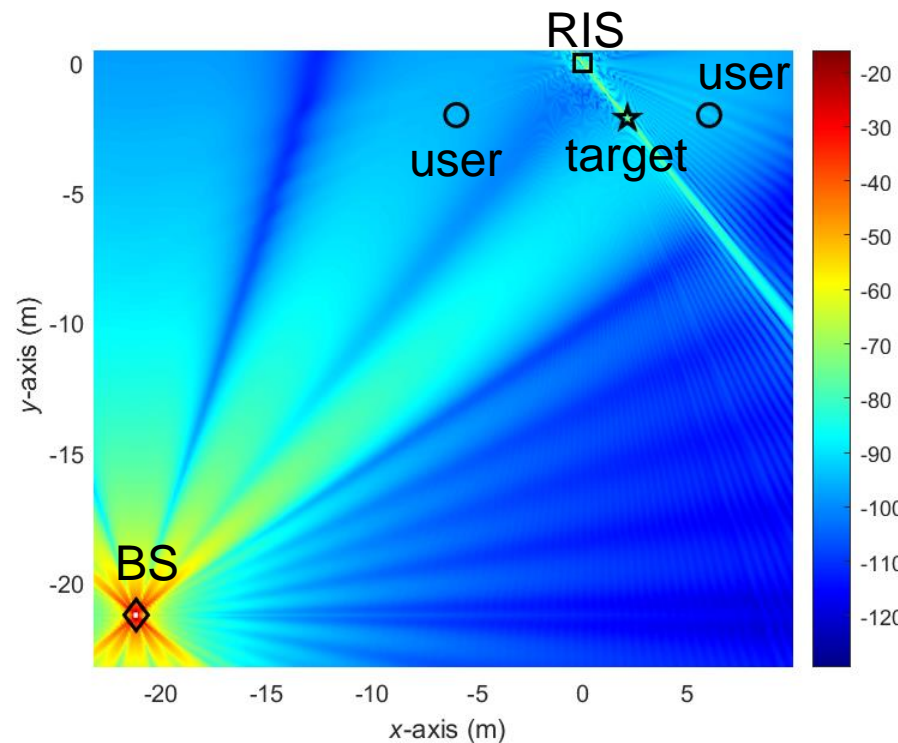
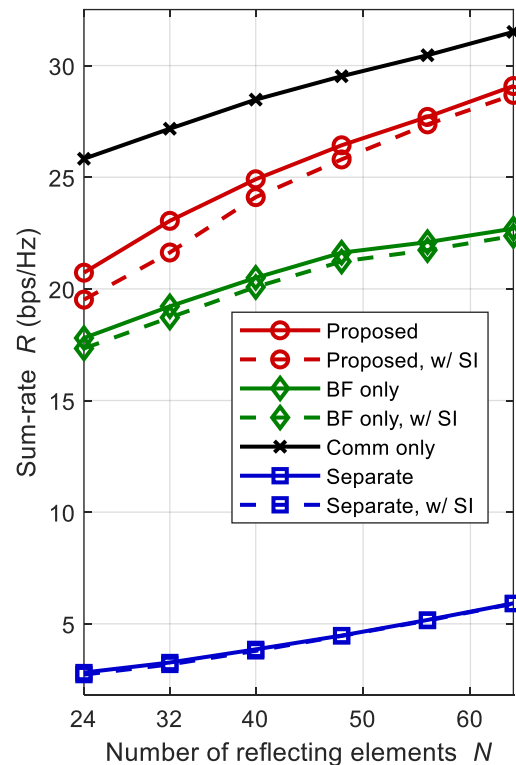
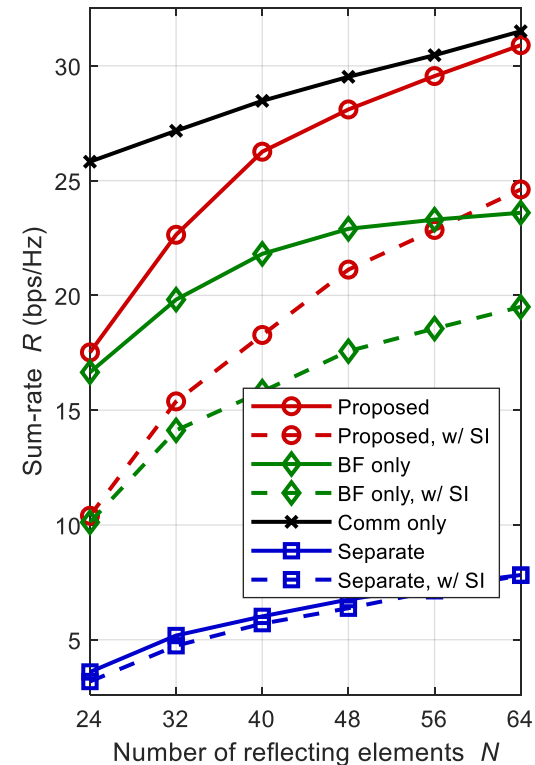


Fig. 19. Enhanced beampattern of the RIS-assisted system.

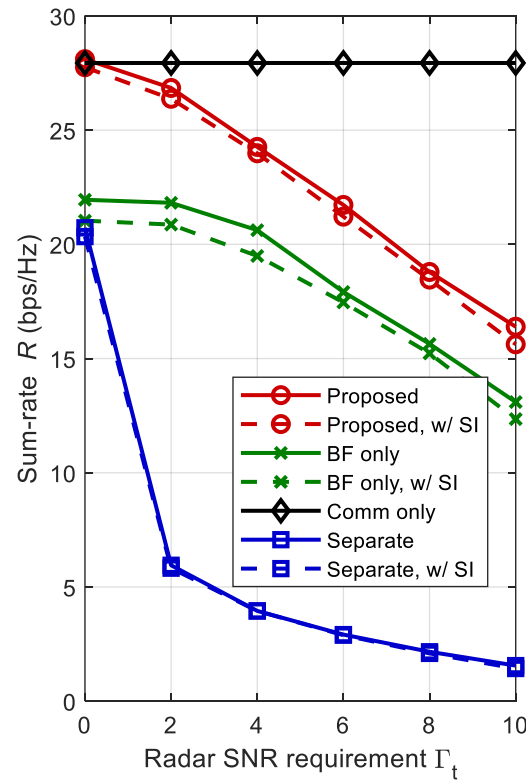


(a) SNR-constrained.

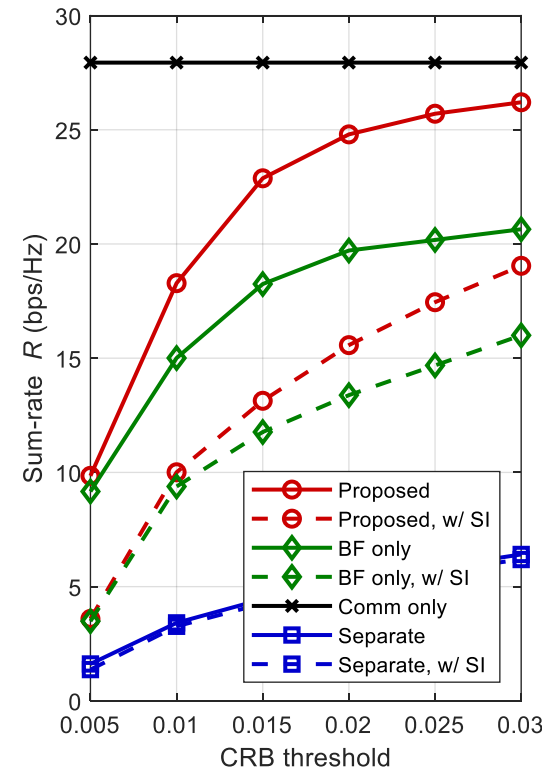


(b) CRB-constrained.

Fig. 20. Sum-rate versus the number of reflecting elements.



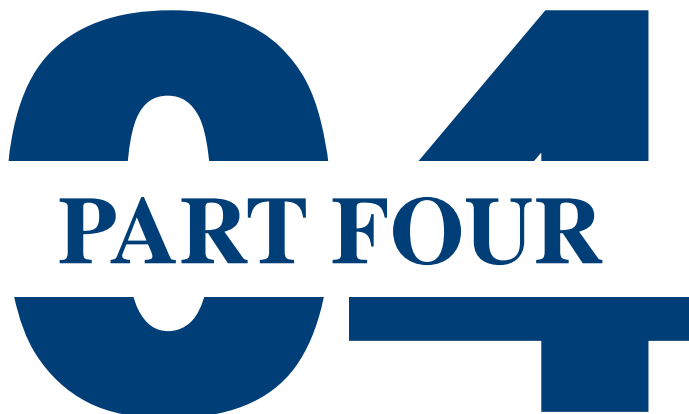
(a) SNR-constrained.



(b) CRB-constrained.

Fig. 21. Impact of radar sensing performance.

PART FOUR

A large, stylized graphic element composed of blue and white shapes. It features a large circle at the top and bottom, with a vertical bar in the center. The word "PART FOUR" is written in a bold, serif font across the central bar.

Conclusions

Future Directions

□ Conclusions

- A general system model for RIS-ISAC systems
- Joint transmit waveform and passive beamforming design
- SNR/CRB-constrained joint beamforming designs

□ Future Directions

- Sensing algorithms based on multipath exploitation
- Near-field communication and sensing
- Wideband waveform design for RIS-ISAC

Related Publications

- [1] **Rang Liu**, M. Li, Y. Liu, Q. Wu, and Q. Liu, “Joint transmit waveform and passive beamforming design for RIS-aided DFRC systems,” *IEEE J. Sel. Topics Signal Process.*, vol. 16, no. 5, pp. 995-1010, Aug. 2022.
- [2] **Rang Liu**, M. Li, H. Luo, Q. Liu, and A. L. Swindlehurst, “Integrated sensing and communication with reconfigurable intelligent surfaces: Opportunities, applications, and future directions,” *IEEE Wireless Commun.*, vol. 30, no. 1, pp. 50-57, Feb. 2023.
- [3] **Rang Liu**, M. Li, Q. Liu, and A. L. Swindlehurst, “SNR/CRB-constrained joint beamforming and reflection designs for RIS-ISAC systems,” *IEEE Trans. Wireless Commun.*, to appear.
- [4] H. Luo, **Rang Liu**, M. Li, and Q. Liu, “RIS-aided integrated sensing and communication: Joint beamforming and reflection design,” *IEEE Trans. Veh. Technol.*, vol. 72, no. 7, pp. 9626-9630, Jul. 2023.
- [5] H. Luo, **Rang Liu**, M. Li, Y. Liu, and Q. Liu, “Joint beamforming design for RIS-assisted integrated sensing and communication systems,” *IEEE Trans. Veh. Technol.*, vol. 71, no. 12, pp. 13393-13397, Dec. 2022.
- [6] H. Zhang, **Rang Liu**, M. Li, W. Wang, and Q. Liu, “Joint sensing and communication optimization in target-mounted STARS-assisted vehicular networks: A MADRL approach,” *IEEE Trans. Veh. Technol.*, to appear.
- [7] Q. Zhu, M. Li, **Rang Liu**, and Q. Liu, “Cramer-Rao bound optimization for active RIS-empowered ISAC systems,” *IEEE Trans. Wireless Commun.*, major revision.
- [8] Q. Zhu, M. Li, **Rang Liu**, and Q. Liu, “Joint transceiver beamforming and reflecting design for active RIS-aided ISAC systems,” *IEEE Trans. Veh. Technol.*, vol. 72, no. 7, pp. 9636-9640, Jul. 2023.
- [9] J. Chu, Z. Lu, **Rang Liu**, M. Li, and Q. Liu, “Joint beamforming and reflection design for secure RIS-ISAC systems,” *IEEE Trans. Veh. Technol.*, to appear.

Acknowledgements



Ming Li



A. Lee Swindlehurst



Yang Liu



Qingqing Wu



Qian Liu



THANK YOU!

Q & A

The source codes can be found at <https://rangliu0706.github.io/>